JACS
JOURNAL OF THE AMERICAN CHEMICAL SOCIETY
pubs.acs.org/JACS
Article

Controlling One- or Two-Electron Oxidation for Selective Amine Functionalization by Alternating Current Frequency

Disni Gunasekera,[§] Jyoti P. Mahajan,[§] Yanick Wanzi, Sachini Rodrigo, Wei Liu, Ting Tan, and Long Luo*

Cite This: J. Am. Chem. Soc. 2022, 144, 9874–9882
Read Online
ACCESS | Metrics & More | Article Recommendations | Supporting Information

ABSTRACT: Here, we report a unique electrosynthetic method that enables the selective one-electron oxidation of tertiary amines to generate α-amino radical intermediates over two-electron oxidation to iminium cations, providing easy access to arylation products by simply applying an optimal alternating current (AC) frequency. More importantly, we have discovered an electrochemical descriptor from cyclic voltammetry studies to predict the optimal AC frequency for various amine substrates, circumventing the time-consuming trial-and-error methods for optimizing reaction conditions. This new development in AC electrolysis provides an alternative strategy to solving challenging chemoselectivity problems in synthetic organic chemistry.

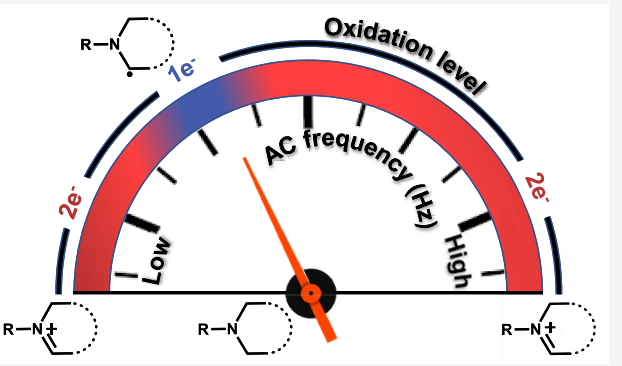

INTRODUCTION

Controlling the degree of oxidation or reduction of substrates is critical to achieving the desired chemical transformation in organic synthesis. In the past decade, electroorganic synthesis has attracted significant attention because it allows for, in principle, straightforward and accurate control over the redox transformations of a substrate by selecting the proper electrode potentials.[1−5] Under typical direct electrolysis conditions, multielectron oxidation or reduction of substrates often takes place. For example, amine substrate **I** is prone to be oxidized by two electrons to *N*-acyl-iminium cation species **II**, which can be later trapped by nucleophiles such as MeOH and H_2O (Figure 1A). Mediated electrolysis is a common strategy to limit multielectron oxidation or reduction in organic electrosynthesis.[6−10] In mediated electrolysis, the electron transfer step is shifted to a homogeneous process that involves an electrochemically generated reagent that serves as a so-called "mediator". The mediator engages in a reversible single-electron redox cycle initiated at the electrode, followed by single-electron transfer (SET) with the substrate (Figure 1B). This strategy provides access to the reactive intermediates formed by the SET events with substrates. For example, Ye and co-workers recently demonstrated using 2,2,6,6-tetramethylpiperidinooxy (TEMPO) as a mediator to perform one-electron oxidation of **I** to **III**, providing access to amino radicals after deprotonation of **III** for radical−radical cross-coupling reaction (Figure 1B).[7]

More recently, AC electrolysis, where the flow of charge periodically changes direction, started to gain interest in the electroorganic synthesis community.[11−19] One of the experimentally observed properties of AC electrolysis is its ability to reduce overoxidation/reduction products without using any mediators relative to its direct current (DC) counterpart.[16] For example, Hilt et al.[13] demonstrated that AC electrolysis solved the problem of the overoxidation of disulfides to oxo species and over-reduction of disulfides to unidentified black precipitate in synthesizing unsymmetrical disulfides by an electrochemical sulfur−sulfur bond metathesis reaction. More recently, Baran et al.[20] presented chemoselective reduction of phthalimides to partially reduced hemiaminal or fully reduced lactam by applying different AC waveforms, which cannot be achieved by DC electrolysis, either. Despite these exciting findings, the mechanisms behind the controlled oxidation or reduction of substrates during AC electrolysis remain unclear. Due to the lack of mechanistic understanding, one must go through a time-consuming reiterative trial-and-error process to discover the optimal AC electrolysis conditions.

Here, we report a mechanism by which AC electrolysis controls the one- or two-electron oxidation of amines to amino radicals or iminium cations, enabling selective α-amine functionalization by simply adjusting the AC frequency. In our model reaction using tertiary amine and dicyanobenzene as the starting materials, the one- and two-electron oxidation

Received: March 9, 2022
Published: May 27, 2022

https://doi.org/10.1021/jacs.2c02605
J. Am. Chem. Soc. 2022, 144, 9874−9882

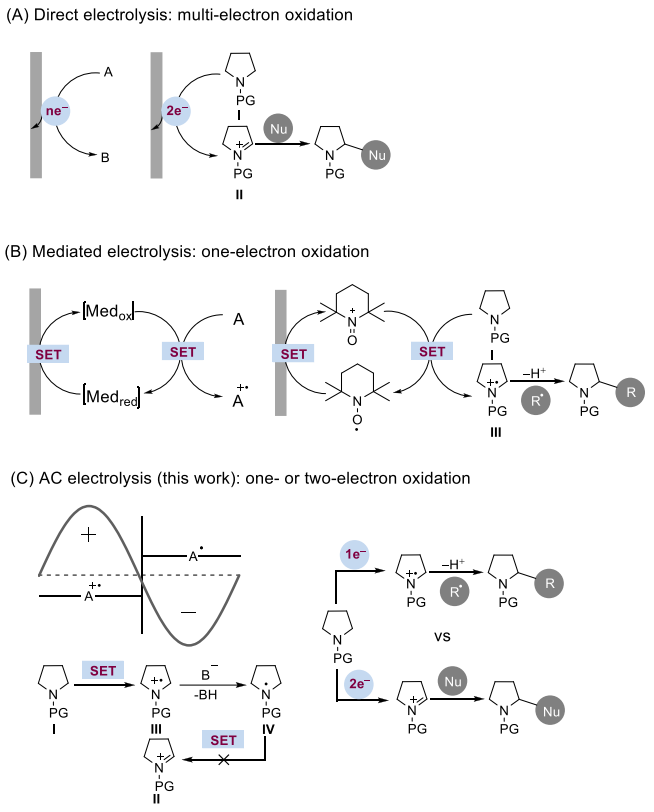

Figure 1. Existing and new strategies for controlling the degree of oxidation of amine substrates during electroorganic synthesis. (A) Direct electrolysis often leads to the two-electron oxidation of amine **I** to iminium cation **II** that can be captured by a nucleophile (Nu). PG stands for protecting group. (B) Mediated electrolysis enables the one-electron oxidation of **I** to cation radical **III**, providing access to amino radical **IV** after the deprotonation of **III** for radical−radical cross-coupling reaction. SET stands for single electron transfer. $[Med_{ox}]$ and $[Med_{red}]$ are the oxidized and reduced forms of the redox mediator, respectively. (C) Alternating current (AC) electrolysis controls one- or two-electron oxidation of amines by managing the redox environment during the deprotonation of **III** to **IV**.

processes of amines compete under paired electrolysis conditions. However, we found that such competition could be controlled by AC electrolysis. The mechanistic study reveals that the degree of amine oxidation is controlled by managing the redox environment where the amino radical cation **III** is deprotonated to amino radical **IV**, utilizing the alternating redox environment of AC electrolysis. When the deprotonation of **III** occurs in an oxidizing environment, **IV** is further oxidized to iminium cation **II** for nucleophilic addition; otherwise, **IV** remains available for radical-based reactions (Figure 1C). Such delicate reaction control requires precise synchronization of the dynamic redox environment and the deprotonation reaction kinetics at the "correct" AC frequency. However, because the deprotonation kinetics of substrates varies significantly, each substrate requires individual reaction optimization, making the empirical trial-and-error reaction optimization approach impractically time-consuming (several days per substrate). Therefore, we developed a convenient electroanalytical method to identify the optimal AC frequency in a few minutes to address it.

RESULTS AND DISCUSSION

In this study, our model reaction is the α-amino C−H arylation reaction, which was first discovered by MacMillan and co-workers using the strategy of accelerated serendipity. This reaction was initially accomplished by photoredox catalysis.[21] We selected this model reaction for two reasons. First, it can be completed by electrochemically oxidizing amine **1** to amine radical cation **3** and reducing 1,4-dicyanobenzene **2** to the corresponding arene radical anion **6** at electrodes (rather than via SET with a photoredox catalyst). The C−H bonds adjacent to the nitrogen atom in **3** are weakened and undergo deprotonation by a base, $\mathbf{B}^-$ such as NaOAc, to give α-amino radical **4**. A radical−radical coupling reaction between intermediates **4** and **6** yields the aromatized benzylic amine product **1a** after the elimination of CN^- (one-electron oxidation (arylation) pathway in Figure 2). Second, unlikely

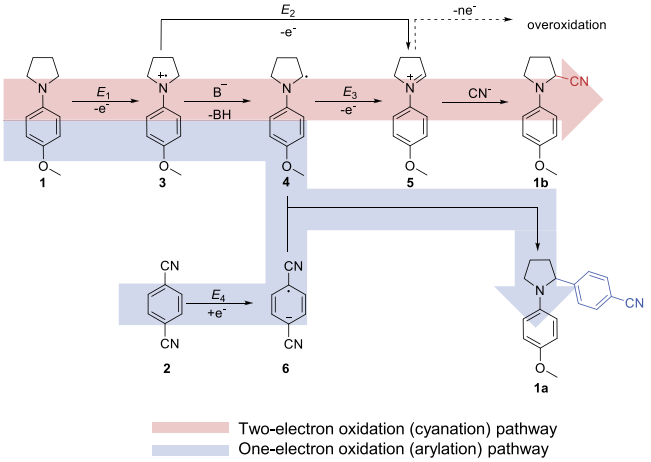

Figure 2. One- and two-electron oxidation pathways during electrochemical α-amino C−H functionalization reactions. One-electron oxidation pathway leads to the arylation product **1a**, while the two-electron oxidation pathway results in the cyanation product **1b**.

photoredox catalysis, electrosynthesis produces a significant amount of cyanation byproduct **1b** because of the over-oxidation of **1** to iminium cation **5** (the two-electron oxidation (cyanation) pathway in Figure 2), enabling us to study how AC electrolysis alters the degree of amine oxidation and controls product selectivity.

First, we carried out the model reaction using a DC electrolysis setup where **1** was oxidized at a carbon anode and **2** was reduced at a carbon cathode to initiate the reaction (Figure S1). Figure 3A shows the isolated yields of **1a** and **1b** at an applied voltage from 2 to 4 V. A mixture of arylation and cyanation products were observed in all cases. At 2.5 V, the best overall conversion of 70% was attained with 30% arylation and 40% cyanation products (**1a**/**1b** = 0.7). After lowering the voltage to 2.0 V, the product selectivity did not show any obvious changes (**1a**/**1b** = 0.8), suggesting that the lowered voltage does not favor the one-electron oxidation pathway over the two-electron one. At high voltages of 3.0 and 4.0 V, the product selectivity slightly shifted to the two-electron oxidation product **1b** (**1a**/**1b** = ∼0.4−0.5), and the overall conversion dropped to ∼50% due to further oxidation of **1** by multiple electrons.

The inevitable two-electron oxidation of amine **1** to iminium **5** and the consequent formation of cyanation product **1b**

https://doi.org/10.1021/jacs.2c02605
J. Am. Chem. Soc. 2022, 144, 9874−9882

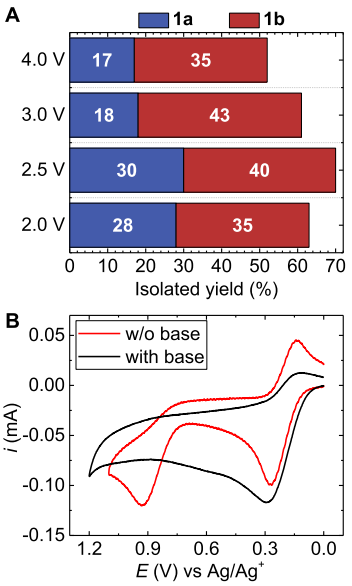

Figure 3. (A) Isolated yields of arylation and cyanation products (blue, **1a**; red, **1b**) using DC electrolysis at different cell voltages. (B) Cyclic voltammograms of **1** in the presence (black) and absence (red) of the base, NaOAc, in *N*,*N*-dimethylacetamide (DMA) containing 0.1 M $LiClO_4$. Scan rate: 1 V/s.

during DC electrolysis can be explained by the cyclic voltammograms (CVs) of **1** collected in the absence and presence of the base, NaOAc, in Figure 3B. Without NaOAc, the CV of **1** (red curve) clearly shows two well-separated anodic peaks. The peak at E_1 = ~0.3 V vs Ag/Ag^+ belongs to the reversible single-electron oxidation of amine **1** to its corresponding cation radical **3**, and the other one at E_2 = ~0.9 V arises from the further oxidation of **3** to **5** by another electron. However, when NaOAc was added, the anodic peak at 0.9 V shifted negatively and merged with the 0.3 V peak (black curve), indicating that one- and two-electron oxidation of **1** can take place under similar potentials. The drastically lowered potential for the second-electron oxidation of **1** in the presence of NaOAc is because iminium cations are generated via the low-potential α-amine radical route ($E_3 < E_2$, Figure 2).[22] As a result, the arylation product **1a** is always accompanied by the cyanation product **1b** under DC electrolysis, regardless of the applied voltage.

Next, we tested AC electrolysis for its effect on product selectivity. During AC electrolysis, the oxidation of **1** and the reduction of **2** occurred sequentially at the same electrode driven by the alternating voltage polarity. Other reaction conditions, including electrodes, electrolytes, and chemical reagents, were identical to the DC electrolysis conditions (Figure S2). We applied sine waveforms with a frequency from 1 to 30 Hz at a fixed AC peak amplitude of 2.5 V. This amplitude was calculated from the potential difference between the oxidation peak of **1** (0.28 V) and the reduction peak of **2** (−2.22 V) in the CVs after *iR* drop correction (Figures S4−S6). Figure 4A shows the product yields and selectivity for DC and AC electrolysis. All AC experiments exhibited a higher selectivity toward the one-electron oxidation pathway (arylation) product **1a** than DC electrolysis, meaning a reduced degree of amine oxidation. At 10 Hz, we observed the maximum yield of 68% for **1a** and the biggest 6-fold selectivity improvement toward **1a** over DC electrolysis (**1a**/**1b** = 4.3 vs 0.7). Under an optimal frequency of 10 Hz, the faradaic efficiency for synthesizing **1a** is 4.4% (see the Supporting Information (SI)).

To understand the AC frequency-dependent product selectivity, we conducted the following experiments to examine the time-resolved amine oxidation behavior. The CVs of **1** were acquired in the presence (black) and absence (red) of NaOAc at different scan rates from 0.02 to 20 V/s (Figure 4B). As previously discussed, **1** undergoes a reversible one-electron redox cycle in the absence of NaOAc, so its anodic peak current (i_0) is an ideal reference of a one-electron oxidation process. After introducing NaOAc to the reaction, the two-electron oxidation of **1** becomes possible at low potentials (<0.6 V). If two-electron oxidation does happen, the anodic peak current (i_1) would be larger than i_0; otherwise, $i_1 = i_0$. By varying the scan rate, we can control the oxidation time (t_{ox}): the higher scan rate, the shorter t_{ox}. In this study, t_{ox} is defined as the time to scan the electrode potential from the onset potential where the oxidation of **1** starts to the anodic peak potential. For example, at a scan rate of 0.02 V/s, t_{ox} is ~8 s and i_1 is approximately twice of i_0 (Figure 4B), suggesting that two-electron oxidation of **1** is dominant for t_{ox} = 8 s. Interestingly, the difference between i_1 and i_0 decreases with increasing scan rate, suggesting that the two-electron oxidation of **1** is suppressed as t_{ox} is shortened. At 5 V/s or t_{ox} = ~45 ms, i_1 became equal to i_0 and part of the CV curve overlapped with the reference CV (red curve), meaning that only one-electron transfer occurred during the 45 ms long anodic potential scan. Recall that the second-electron oxidation of **1** at low potentials is achievable only after deprotonation of **3** to **4**. Therefore, when t_{ox} is short, the second-electron oxidation is hindered possibly due to the slow deprotonation of **3**, resulting in such t_{ox}-dependent oxidation behavior.

On the basis of the CV results above, we propose the following mechanism for the product selectivity change during AC electrolysis: due to the slow deprotonation of **3**, a portion of **3** formed in the positive half-cycle of AC waveform cannot be immediately deprotonated and thus stays intact until the subsequent negative half-cycle. In the reducing environment of the negative half-cycle, deprotonation continues but the further oxidation of the deprotonated product **4** to **5** is prohibited, thereby shifting the product selectivity toward **1a** (Figure 4C). According to the CV data, **3** can be hardly deprotonated to **4** and then oxidized to **5** within ~45 ms. Thus, the AC frequency that provides t_{ox} of 45 ms (i.e., f_{pred} = 11 Hz, see Figure S7) should result in the highest selectivity toward **1a**. The f_{pred} of 11 Hz from the CV measurements is in excellent agreement with the experimentally observed optimal frequency (f_{exp}) of 10 Hz. At even higher frequencies such as 20 or 30 Hz, the deprotonation of **3** might not finish in one AC period and thus is carried over to the following AC period, resulting in deprotonation in an oxidizing environment again and an increased yield for two-electron oxidation product **1b**.

The intriguing agreement between the CV-derived frequency (f_{pred}) and f_{exp} led us to think if we can predict f_{exp} for other amine substrates from their CVs. It is critical to be able to predict f_{exp} because it takes several days to determine the optimal frequency for one substrate using the trial-and-error method as every reaction requires a separate power supply and takes more than 24 h to complete. To test this idea, we collected the CVs of a variety of amines, including *N*-aryl pyrrolidines bearing electron-donating and withdrawing groups (**7**−**18**), *N*-aryl piperidine (**19**), *N*-aryl tetrahydroisoquinoline (**20**), and aliphatic amine (**32**). These amines showed similar

https://doi.org/10.1021/jacs.2c02605
J. Am. Chem. Soc. 2022, 144, 9874−9882

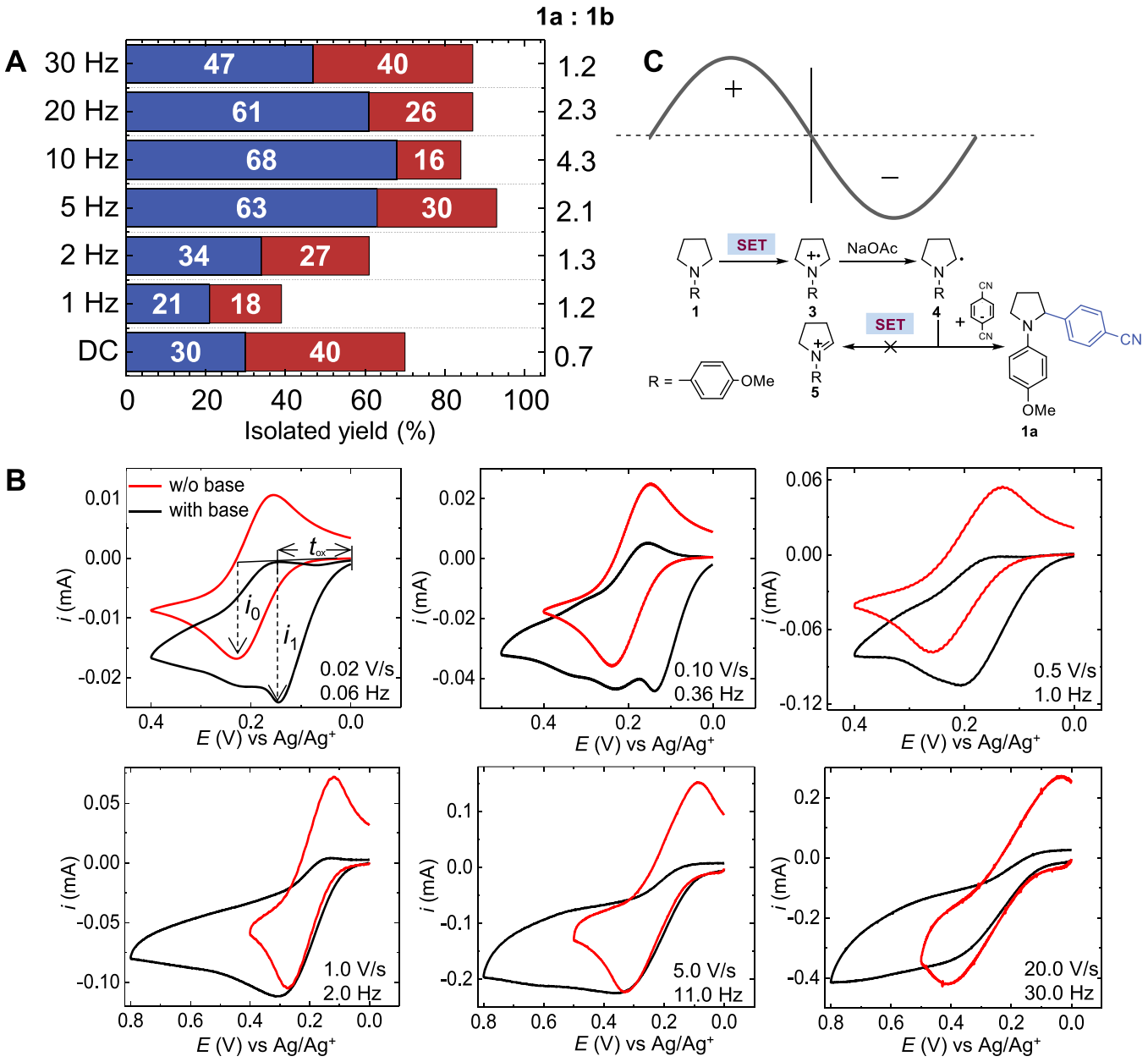

Figure 4. (A) Isolated yields and selectivity of arylation and cyanation products (**1a** and **1b**) at different AC frequencies from 1 to 30 Hz. (B) Cyclic voltammograms of **1** in the presence and absence of NaOAc in DMA containing 0.1 M $LiClO_4$ at different scan rates and their equivalent AC frequencies. (C) Proposed mechanism for the reduced degree of amine oxidation during AC electrolysis.

scan-rate dependent CVs as **1** (Figures S16−S29 and S41): the ratio between i_1 and i_0 ($|i_1/i_0|$) generally decreases with increasing scan rate, suggesting the slow deprotonation of amine cation radicals by NaOAc is true for all tertiary amines. We determined f_{pred} from the scan rate that produced $|i_1/i_0|$ that is most close to one (Figures S7 and S9C).

In parallel, we experimentally identified f_{exp} via conventional reaction optimization (i.e., running reactions at different AC frequencies and determining the selectivity from crude NMR, Figures S9−S11). Figure 5A shows the excellent agreement between f_{exp} and f_{pred} for various amines, confirming the predictive power of the simple electrochemical descriptor (i.e., $|i_1/i_0|$) in finding the optimal frequency for selective arylation over cyanation. We also attempted to understand the dispersed f_{exp} values (by 2 orders of magnitude) for different amines from the calculated pK_a values of their corresponding cation radicals (Figures S12 and S13, Table S1). However, we did not find any obvious correlation between f_{exp} and pK_a (Figure S13), suggesting that the deprotonation rate is not solely determined by the acidity of these cation radical intermediates. We further varied the cyanoaromatic coupling partners, including 1,2-dicyanobenzene (**35**), ethyl 4-cyanobenzoate (**36**), 4,4′-biphenylcarbinitrile (**37**), and 2,5-dicyanotoluene (**38**) and bases, including LiOAc, CsOAc, NaOMe, NaOH, Na_2CO_3, and $NaHCO_3$ to examine their effects on f_{exp}. Cyanoaromatics **35**−**38** show similar reversible redox behaviors with a reduction potential of ∼−2 V vs Ag/Ag^+ as **2** (Figure S44) and have little impact on f_{exp} because they are not involved in the deprotonation of **3**. In contrast, Figure 5B shows that base strongly influences f_{exp} and the CV-based method accurately predicts f_{exp} (Figures S45−S50), further supporting our proposed mechanism that the deprotonation step plays an

https://doi.org/10.1021/jacs.2c02605
J. Am. Chem. Soc. 2022, 144, 9874−9882

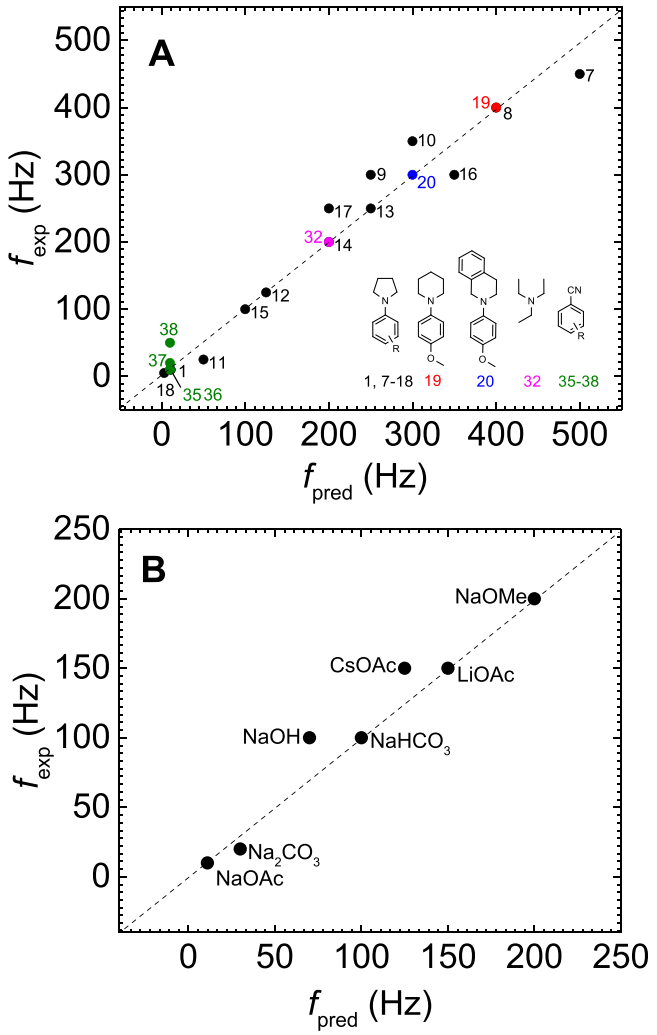

Figure 5. (A) Plot of experimentally determined optimal frequency (f_{exp}) vs predicted optimal frequency (f_{pred}) for various tertiary amines and cyanoaromatics. (B) Plot of f_{exp} vs f_{pred} for **1** with different bases.

essential role in controlling the degree of amine oxidation and product selectivity during AC electrolysis.

To confirm the one-electron oxidation of amines to α-amine radicals at the optimal frequency, we performed the radical trapping experiment on amine **1** and **20**. Five equiv of TEMPO was added to the reaction mixture under the optimal AC electrolysis conditions. We did not observe the formation of arylation product **1a** or **20a**. However, the formation of the TEMPO-adduct of **1** and **20** (Figures S14 and S15) indicates that this reaction proceeds via α-amine radical pathway.

Finally, we evaluated the substrate scope and compared the product selectivity between AC and DC electrolysis in Figure 6. For all substrates, we performed AC electrolysis under f_{exp} and DC electrolysis. For *N*-aryl pyrrolidine bearing electron-donating groups such as methyl, tertiary butyl, 2,6-dimethyl, indane, dioxole, ethyl acetate, and phenyl, the arylation product yields were significantly improved from 5 to 30% under DC electrolysis to 43−68% under AC electrolysis (**1a, 7a-14a**) while the cyanation product yields dropped from 11 to 40 and 0−38% (**1b, 7b−14b**). The product selectivity shifted from the cyanation products under DC electrolysis to the arylation products under AC electrolysis. The *N*-aryl pyrrolidine substituted with electron-withdrawing groups such as F, Cl, and Br also afforded one-electron transfer products (**15a−17a**) with greater selectivity and yields under AC electrolysis than the DC counterpart. In the case of *N*-aryl pyrrolidine without any substituent on ring (**18**) afforded poor yield (<20%) and selectivity under both electrolysis conditions (**18a** and **18b**). The reaction of six-membered cyclic amine, *N*-aryl piperidine **19**, with **2** under both AC and DC electrolysis conditions provided poor yield for **19a** and **19b**, possibly because the impaired overlap between the lone pair of amine and the unpaired electron at the α-carbon significantly destabilizes the α-amino radical intermediate.[7]

Encouraged by the broad generality of our approach on five-membered cyclic amines, we tested it on another class of tertiary amines, *N*-aryl tetrahydroisoquinoline. Tetrahydroisoquinoline alkaloids are an important class of bioactive natural products and display a myriad of biological activities.[23,24] *N*-aryl ring bearing electron-donating and electron-withdrawing groups such as methoxy, fluoro, dioxine, dimethyl, trifluoromethyl (**20−26**), and *N*-benzyl (**27**) all afforded arylated and cyanation products (**20a−27a** and **20b−27b**). Under DC electrolysis, the formation of cyanation product was predominantly observed in good yield 36−63% because the benzylic position is prone to overoxidation to form iminium cation.[25−27] Under AC electrolysis, arylation product formation significantly improved to good/moderate yields of 26−51%. However, the cyanation product yields were comparable to the DC electrolysis results, even though the CV data in Figures S29−S36 predicts that the two-electron oxidation of *N*-aryl tetrahydroisoquinolines should be largely reduced at f_{exp}, like the *N*-aryl pyrrolidine oxidation. A possible explanation for the discrepancy is that there are alternative pathways to generate iminium cations that does not require NaOAc, for example, via deprotonation by in situ generated CN^-[27] or dicyanobenzene **2**.[28] This explanation is in part supported by the formation of arylation and cyanation products at moderate yields for tetrahydroisoquinoline **20** even in the absence of NaOAc (Table S2).

We have also identified the tertiary amine-containing heteroaromatic rings as a suitable class of substrates (**28−31**). Various *N*-benzyl/alkyl thienopyridines containing susceptible functional groups such as ester and allyl were tested. The reaction of **28** with benzonitrile **2** under DC electrolysis provided poor yield and selectivity for arylation product **28a** relative to cyanation product **28b**. In contrast, the yield of **28a** improved from 17 to 54% under AC conditions. Notably, the arylation occurred regioselectively at cyclic amine and the benzylic methylene group remained intact. In the presence of ester (**29**), DC electrolysis did not yield any products. This situation was altered when AC was applied, delivering both products at a yield of 31% for **29a** and 37% for **29b**. In the case of *N*-allyl group, significant enhancement in yield and selectivity was not observed (**30a** and **30b**). For late-stage functionalization of antiplatelet drug Ticlopidine **31**, the arylation and cyanation product yields (**31a** and **31b**) slightly increased under AC electrolysis.

The tertiary aliphatic amines were also investigated. DC electrolysis did not furnish any arylation or cyanation products. In contrast, one-electron oxidation arylation product exclusively formed under AC conditions in moderate yields 28−39% (**32a−34a**). Dealkylation of aliphatic amines under electrooxidative conditions is the possible reason for their moderate yields.[29,30] Tertiary amines containing strong

https://doi.org/10.1021/jacs.2c02605
J. Am. Chem. Soc. 2022, 144, 9874−9882

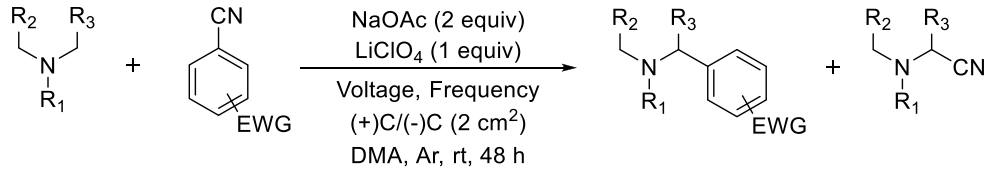

N-Aryl Pyrrolidines

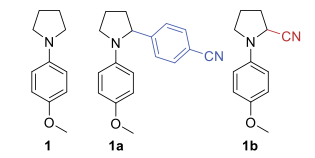

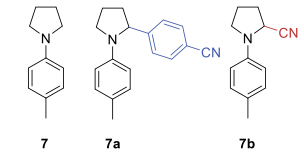

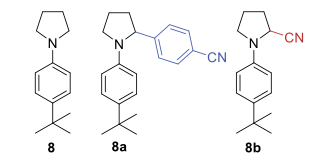

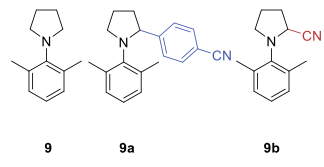

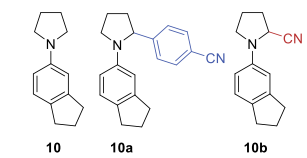

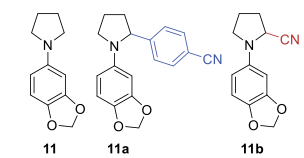

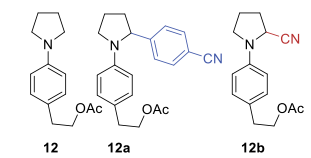

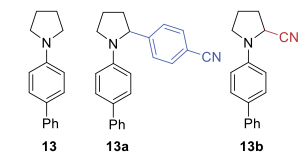

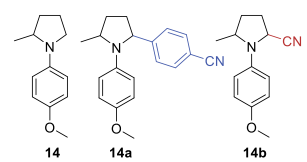

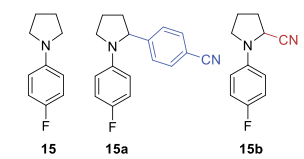

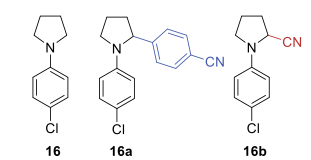

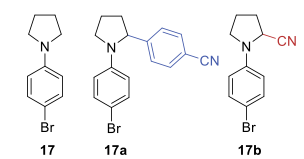

N-Aryl Tetrahydroisoquinolines

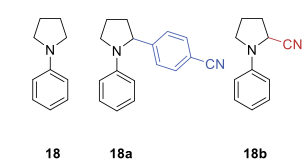

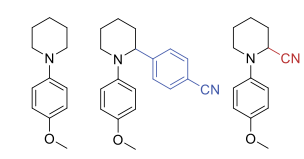

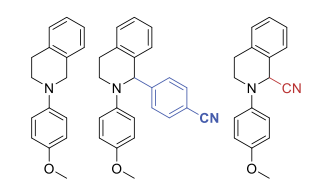

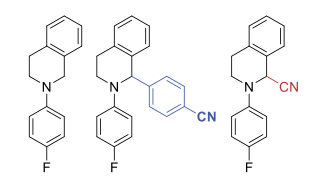

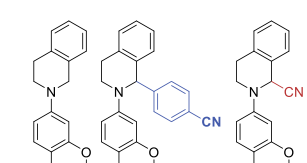

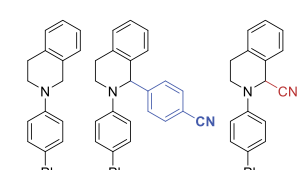

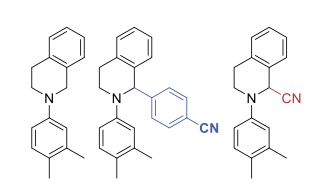

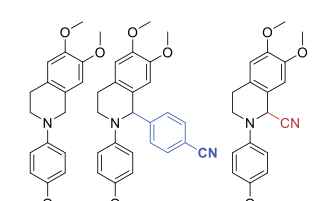

Figure 6. continued

https://doi.org/10.1021/jacs.2c02605
J. Am. Chem. Soc. 2022, 144, 9874−9882

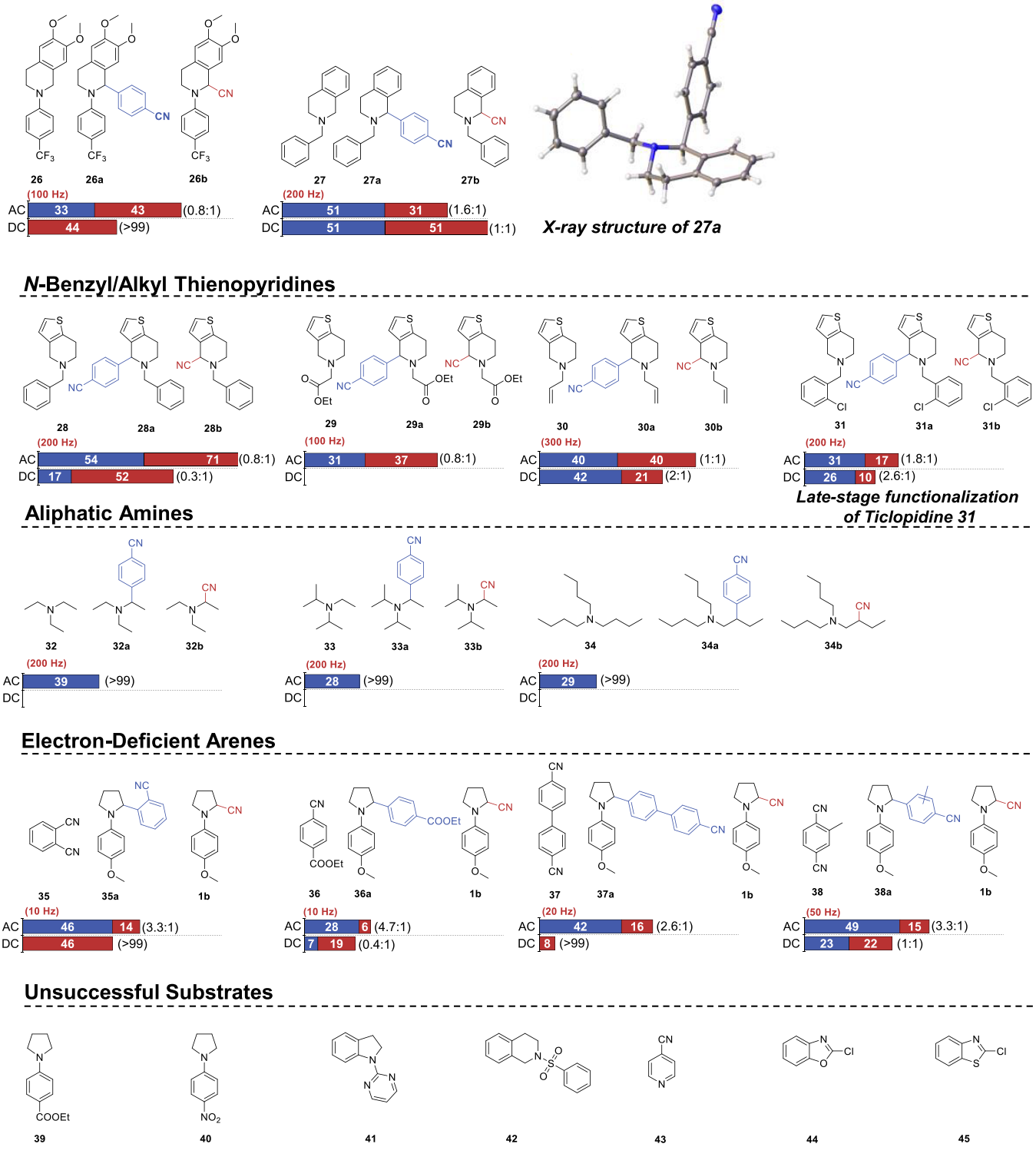

Figure 6. Substrate scope and product selectivity comparison between AC and DC electrolysis. Note: **18b** and **19b** were characterized using high-resolution mass spectrometry. Yields of **30a** and **30b** were determined using ^{1}H NMR of the purified inseparable compounds. Regioisomers of **38a** were formed in 1:0.6 ratio. The experimental frequency for each substrate is provided in parentheses. All yields were calculated considering 0.5 mmol of 1,2-dicyanobenzene as the limiting reagent.

electron-withdrawing functional groups such as ester and nitro (**39**–**40**), pyrimidinyl (**41**), and benzenesulfonyl (**42**) did not result in any products (Figure 6). The unavailability of nitrogen lone pair electrons due to strong electron-withdrawing effect makes it difficult to oxidize these amines to stable radical cation intermediates.

Moreover, the substrate scope for aromatic partner **2** was also explored. Cyanoaromatics **35**–**38** successfully underwent coupling with **1** to furnish arylated products in moderate to good yields (**35a**–**38a**). In contrast, the product involving two-electron transfer was predominantly obtained in most cases in moderate to low yields (**1b**) under DC electrolysis. The

https://doi.org/10.1021/jacs.2c02605
J. Am. Chem. Soc. 2022, 144, 9874−9882

arylated product **38a** was a 1:0.6 mixture of two isomers due to a lack of regioselectivity in elimination of CN^- group in reaction. The coupling of **1** with electron-deficient heteroaromatics such as 4-cyanopyridine (**43**), 2-chlorobenzthiozole (**44**), and 2-chlorobenzoxazole (**45**) were not successful using AC or DC electrolysis (Figure 6), possibly because of the poor stability of their anion radicals. Compared with the TEMPO-mediated electrolysis method developed by Ye and coworkers,[7] our AC electrolysis method exhibits similar substrate scope and yields, which is not surprising because both methods rely on limiting the oxidation level of amines to generate the critical intermediate of α-amine radicals but via different approaches.

CONCLUSIONS

In conclusion, we have reported a mechanism by which AC electrolysis controls the one- or two-electron oxidation of amines to amino radicals or iminium cations, enabling selective α-amine functionalization by adjusting the AC frequency. We found that the selective one-electron oxidation of amines to amino radicals was achieved by providing a reducing environment for the deprotonation of amino radical cations. We have also developed a convenient electroanalytical method to identify the optimal AC frequency that maximizes the arylation product of the one-electron oxidation pathway, eliminating the time-consuming trial-and-error approach in conventional AC electrolysis condition optimization. We envision that this highly efficient and unique AC electrolysis protocol can be applied to achieve unique reactivities in synthetic and medicinal chemistry.

ASSOCIATED CONTENT

Supporting Information

The Supporting Information is available free of charge at https://pubs.acs.org/doi/10.1021/jacs.2c02605.

Discussions of experimental procedures, determination of the optimal voltage and frequency for each substrate, method validation, pK_a calculations, X-ray crystallography data, and full characterization data, figures of photographs of the experimental setup, CV data, plot of the positive plateau current vs scan rate, Nyquist plot, peak current ratio, current−time trace, NMR spectra, ^{1}H NMR selectivity, thermodynamic cycle, plot of optimal AC frequencies and calculated pKa values for various *N*-aryl pyrrolidines, and HRMS spectra, tables of pK_a values of *N*-aryl pyrrolidines cation radicals, data from other experiments, and X-ray crystallographic data and structure refinement (PDF)

Accession Codes

CCDC 2150591 contains the supplementary crystallographic data for this paper. These data can be obtained free of charge via www.ccdc.cam.ac.uk/data_request/cif, or by emailing data_request@ccdc.cam.ac.uk, or by contacting The Cambridge Crystallographic Data Centre, 12 Union Road, Cambridge CB2 1EZ, UK; fax: +44 1223 336033.

AUTHOR INFORMATION

Corresponding Author

Long Luo − *Department of Chemistry, Wayne State University, Detroit, Michigan 48202, United States;* orcid.org/0000-0001-5771-6892; Email: long.luo@wayne.edu

Authors

Disni Gunasekera − *Department of Chemistry, Wayne State University, Detroit, Michigan 48202, United States;* orcid.org/0000-0002-6964-8337

Jyoti P. Mahajan − *Department of Chemistry, Wayne State University, Detroit, Michigan 48202, United States;* orcid.org/0000-0002-6071-6348

Yanick Wanzi − *Department of Chemistry, Wayne State University, Detroit, Michigan 48202, United States*

Sachini Rodrigo − *Department of Chemistry, Wayne State University, Detroit, Michigan 48202, United States;* orcid.org/0000-0002-6828-6637

Wei Liu − *Laboratory of Theoretical and Computational Nanoscience, CAS Center for Excellence in Nanoscience, National Center for Nanoscience and Technology, Chinese Academy of Sciences, Beijing 100190, China*

Ting Tan − *Laboratory of Theoretical and Computational Nanoscience, CAS Center for Excellence in Nanoscience, National Center for Nanoscience and Technology, Chinese Academy of Sciences, Beijing 100190, China;* orcid.org/0000-0003-3129-8113

Complete contact information is available at: https://pubs.acs.org/10.1021/jacs.2c02605

Author Contributions

[§]D.G. and J.P.M. contributed equally to this work. The manuscript was written through the contributions of all authors. All authors have given approval to the final version of the manuscript.

Notes

The authors declare no competing financial interest.

ACKNOWLEDGMENTS

D.G., J.P.M., and L.L. gratefully acknowledge support from NIH (1R35 GM142590-01), the start-up funds, the Thomas C. Rumble University Graduate Fellowship, and the Faculty Competition for Postdoctoral Fellows ward from Wayne State University. The authors would like to thank Cassandra Ward (the Lumigen Instrument Center) for assistance with X-ray crystallographic analysis.

REFERENCES

(1) Yan, M.; Kawamata, Y.; Baran, P. S. Synthetic Organic Electrochemistry: Calling All Engineers. *Angew. Chem., Int. Ed.* **2018**, *57* (16), 4149−4155.

(2) Yan, M.; Kawamata, Y.; Baran, P. S. Synthetic Organic Electrochemical Methods Since 2000: On the Verge of a Renaissance. *Chem. Rev.* **2017**, *117* (21), 13230−13319.

(3) Yoshida, J.-i.; Kataoka, K.; Horcajada, R.; Nagaki, A. Modern Strategies in Electroorganic Synthesis. *Chem. Rev.* **2008**, *108* (7), 2265−2299.

(4) Pletcher, D. Organic electrosynthesis − A road to greater application. A mini review. *Electrochem. Commun.* **2018**, *88*, 1−4.

(5) Wiebe, A.; Gieshoff, T.; Möhle, S.; Rodrigo, E.; Zirbes, M.; Waldvogel, S. R. Electrifying organic synthesis. *Angew. Chem., Int. Ed.* **2018**, *57* (20), 5594−5619.

(6) Lennox, A. J. J.; Goes, S. L.; Webster, M. P.; Koolman, H. F.; Djuric, S. W.; Stahl, S. S. Electrochemical Aminoxyl-Mediated α-Cyanation of Secondary Piperidines for Pharmaceutical Building Block Diversification. *J. Am. Chem. Soc.* **2018**, *140* (36), 11227−11231.

(7) Ma, Y.; Yao, X.; Zhang, L.; Ni, P.; Cheng, R.; Ye, J. Direct Arylation of α-Amino C(sp3)-H Bonds by Convergent Paired Electrolysis. *Angew. Chem., Int. Ed.* **2019**, *131* (46), 16700−16552.

(8) Wang, F.; Rafiee, M.; Stahl, S. S. Electrochemical Functional-Group-Tolerant Shono-type Oxidation of Cyclic Carbamates Enabled by Aminoxyl Mediators. *Angew. Chem., Int. Ed.* **2018**, *57* (22), 6686−6690.
(9) Francke, R.; Little, R. D. Redox catalysis in organic electrosynthesis: basic principles and recent developments. *Chem. Soc. Rev.* **2014**, *43* (8), 2492−2521.
(10) Wang, F.; Stahl, S. S. Electrochemical oxidation of organic molecules at lower overpotential: Accessing broader functional group compatibility with electron− proton transfer mediators. *Acc. Chem. Res.* **2020**, *53* (3), 561−574.
(11) Rodrigo, S.; Um, C.; Mixdorf, J. C.; Gunasekera, D.; Nguyen, H. M.; Luo, L. Alternating Current Electrolysis for Organic Electrosynthesis: Trifluoromethylation of (Hetero)arenes. *Org. Lett.* **2020**, *22*, 6719.
(12) Bortnikov, E. O.; Semenov, S. N. Coupling of Alternating Current to Transition-Metal Catalysis: Examples of Nickel-Catalyzed Cross-Coupling. *Journal of Organic Chemistry* **2021**, *86* (1), 782−793.
(13) Sattler, L. E.; Otten, C. J.; Hilt, G. Alternating Current Electrolysis for the Electrocatalytic Synthesis of Mixed Disulfide via Sulfur−Sulfur Bond Metathesis towards Dynamic Disulfide Libraries. *Chem. Eur. J.* **2020**, *26* (14), 3129−3136.
(14) Hilt, G. Basic Strategies and Types of Applications in Organic Electrochemistry. *ChemElectroChem.* **2020**, *7* (2), 395−405.
(15) Schotten, C.; Taylor, C. J.; Bourne, R. A.; Chamberlain, T. W.; Nguyen, B. N.; Kapur, N.; Willans, C. E. Alternating polarity for enhanced electrochemical synthesis. *Reaction Chemistry & Engineering* **2021**, *6* (1), 147−151.
(16) Rodrigo, S.; Gunasekera, D.; Mahajan, J. P.; Luo, L. Alternating current electrolysis for organic synthesis. *Curr. Opin. Electrochem.* **2021**, *28*, 100712.
(17) Fährmann, J.; Hilt, G. Alternating Current Electrolysis as Efficient Tool for the Direct Electrochemical Oxidation of Hydroxamic Acids for Acyl Nitroso Diels−Alder Reactions. *Angew. Chem., Int. Ed.* **2021**, *60* (37), 20313−20317.
(18) Zhong, J.; Ding, C.; Kim, H.; McCallum, T.; Ye, K. Alternating current electrolysis: a photoredox catalysis mimic and beyond. *Green Synthesis and Catalysis* **2022**, *3* (1), 4−10.
(19) Wang, D.; Jiang, T.; Wan, H.; Chen, Z.; Qi, J.; Yang, A.; Huang, Z.; Yuan, Y.; Lei, A. Alternating Current Electrolysis Enabled Formal C-O/O-H Cross-Metathesis of 4-Alkoxy Anilines with Alcohols. *Angew. Chem., Int. Ed.* **2022**, *61* (18), e202201543.
(20) Kawamata, Y.; Hayashi, K.; Carlson, E.; Shaji, S.; Waldmann, D.; Simmons, B. J.; Edwards, J. T.; Zapf, C. W.; Saito, M.; Baran, P. S. Chemoselective Electrosynthesis Using Rapid Alternating Polarity. *J. Am. Chem. Soc.* **2021**, *143* (40), 16580−16588.
(21) McNally, A.; Prier, C. K.; MacMillan, D. W. Discovery of an α-amino C-H arylation reaction using the strategy of accelerated serendipity. *Science* **2011**, *334* (6059), 1114−7.
(22) Novaes, L. F. T.; Ho, J. S. K.; Mao, K.; Liu, K.; Tanwar, M.; Neurock, M.; Villemure, E.; Terrett, J. A.; Lin, S. Exploring Electrochemical C(sp3)−H Oxidation for the Late-Stage Methylation of Complex Molecules. *J. Am. Chem. Soc.* **2022**, *144* (3), 1187−1197.
(23) Faheem; Karan Kumar, B.; Chandra Sekhar, K. V. G.; Chander, S.; Kunjiappan, S.; Murugesan, S. Medicinal chemistry perspectives of 1,2,3,4-tetrahydroisoquinoline analogs − biological activities and SAR studies *RSC. RSC Adv.* **2021**, *11* (20), 12254−12287.
(24) Kaur, P.; Kumar, R. Recent advances in the C(1)-functionalization of tetrahydroisoquinolines via multicomponent reactions. *Chem. Heterocycl. Compd. (N. Y., NY, U. S.)* **2020**, *56*, 422−432.
(25) Xie, W.; Liu, N.; Gong, B.; Ning, S.; Che, X.; Cui, L.; Xiang, J. Electrochemical Cross-Dehydrogenative Coupling of N-Aryl-tetrahydroisoquinolines with Phosphites and Indole. *Eur. J. Org. Chem.* **2019**, *2019* (14), 2498−2501.
(26) Benmekhbi, L.; Louafi, F.; Roisnel, T.; Hurvois, J.-P. Synthesis of Tetrahydroisoquinoline Alkaloids and Related Compounds through the Alkylation of Anodically Prepared α-Amino Nitriles. *Journal of Organic Chemistry* **2016**, *81* (15), 6721−6739.
(27) Louafi, F.; Hurvois, J.-P.; Chibani, A.; Roisnel, T. Synthesis of Tetrahydroisoquinoline Alkaloids via Anodic Cyanation as the Key Step. *Journal of Organic Chemistry* **2010**, *75* (16), 5721−5724.
(28) Stevenson, B. G.; Spielvogel, E. H.; Loiaconi, E. A.; Wambua, V. M.; Nakhamiyayev, R. V.; Swierk, J. R. Mechanistic Investigations of an α-Aminoarylation Photoredox Reaction. *J. Am. Chem. Soc.* **2021**, *143* (23), 8878−8885.
(29) Masui, M.; Sayo, H.; Tsuda, Y. Anodic oxidation of amines. Part I. Cyclic voltammetry of aliphatic amines at a stationary glassy-carbon electrode. *Journal of the Chemical Society B: Physical Organic* **1968**, *0*, 973−976.
(30) Masui, M.; Sayo, H. Anodic oxidation of amines. Part II. Electrochemical dealkylation of aliphatic tertiary amines. *Journal of the Chemical Society B: Physical Organic* **1971**, 1593−1596.

https://doi.org/10.1021/jacs.2c02605
J. Am. Chem. Soc. 2022, 144, 9874−9882